



HAL
open science

Generation of stabilized electrically-induced micro-plasma at the tip of multimaterial optical fibers

Sara Alhomsy, Lionel Teule-gay, Lionel Canioni, Bruno Bousquet, Sylvain Danto

► **To cite this version:**

Sara Alhomsy, Lionel Teule-gay, Lionel Canioni, Bruno Bousquet, Sylvain Danto. Generation of stabilized electrically-induced micro-plasma at the tip of multimaterial optical fibers. *Optical Fiber Technology*, 2023, 81, pp.103508. 10.1016/j.yofte.2023.103508 . hal-04214629

HAL Id: hal-04214629

<https://hal.science/hal-04214629>

Submitted on 22 Sep 2023

HAL is a multi-disciplinary open access archive for the deposit and dissemination of scientific research documents, whether they are published or not. The documents may come from teaching and research institutions in France or abroad, or from public or private research centers.

L'archive ouverte pluridisciplinaire **HAL**, est destinée au dépôt et à la diffusion de documents scientifiques de niveau recherche, publiés ou non, émanant des établissements d'enseignement et de recherche français ou étrangers, des laboratoires publics ou privés.

Generation of stabilized electrically-induced micro-plasma at the tip of multimaterial optical fibers

Sara Alhomsy, Lionel Teule-Gay, Lionel Canioni, Bruno Bousquet, Sylvain Danto*

Institute of Chemistry of the Condensed Matter of Bordeaux (ICMCB), University of Bordeaux, 33608 Pessac.

* Corresponding author: sylvain.danto@u-bordeaux.fr

Abstract

The aim of this work is to optimize the operation of a multimaterial optical fiber device to generate a stabilized electrically-induced micro-plasma. The fiber is composed of a polymer cladding with a central hole surrounded by two cylindrical metal electrodes. When a DC voltage of 1.2 kV is applied between electrodes, an air micro-plasma is generated at the tip of the fiber. In order to stabilize the discharge, studies are focused on the modification of the electrical properties of the fiber tip by covering the electrodes with resistive layers. A comparison between two different layers (semi-conductive and semi-insulating) is shown. Characterizations were also performed for the fiber (head and length), and the plasma (imaging, spatial and temporal stability). The results show the effectiveness of the method to cover at least one of the electrodes by the semi-insulating layer to generate a permanent and stable discharge. In fact, this method allowed to increase considerably the lifetime of our technology and avoid the electric arcs leading to high instabilities. According to the Optical Emission Spectroscopy (OES), the species generated by the fiber-plasma device were identified.

The combination of the characteristics of optical fibers with the properties of plasma allows diverse potential applications, such as gas detection in remote, confined, or harsh environments, high-level disinfection and sterilization of medical equipment or high-quality surface treatment (micrometric scale).

Keywords: Preform-to-fiber drawing, multimaterial optical fiber, air cold micro-plasma, resistive layer, resistive barrier discharge

I Introduction

A new family of hybrid multi-purpose optical fibers composed of conductors, semiconductors and insulators has recently emerged. These multifunctional fibers combining special optical, electrical, or mechanical assets are fabricated using conventional preform-based fiber-processing methods [1-5]. Furthermore, the merge of optical fibers technology and plasmas has a great interest to meet some requirements in the industrial and medical fields, such as the optical diagnostics in remote, confined, or harsh environments [6-10], the treatment of tumors in internal organs (lungs, pancreas, duodenum) [11-13], etc. Here the fibers are commonly used to transmit plasma optical emissions to detectors for various optical diagnostics [6-10]. However, other studies have shown that fibers can not only transmit light but also generate a plasma [11-13]. A micro-plasma jet device is fabricated using a hollow-core optical glass fiber. This device operates with a noble gas as the working gas (helium or argon) and using a high frequency power supply (in the kHz to MHz range). It has a conventional configuration of the Dielectric Barrier Discharge (DBD), as described in [11-13].

Recently, we proposed a new type of optical fibers to generate a micro-plasma, which can operate with air as the working gas and using a DC power supply [14]. A special hollow cylindrical multimaterial fiber structure is fabricated to generate a plasma at its tip. It is composed of a polymer cladding with a central hole surrounded by two cylindrical metal electrodes. When a DC voltage of 1.2 kV is applied between the electrodes, the air plasma at atmospheric pressure is generated. The results shown the efficiency of this device for gas detection [14]. However, due to the high electron-neutral particles collision frequency (10^{11-12} /s), the glow discharge is turned into an electrical arc. The arc is known as a highly unstable discharge, which can reach very high temperatures [15]. Then, it can degrade not only the electrodes but also any surface in contact, which makes it difficult to use for most applications. For that, the main aim of this work is to optimize the operation of our technology by generating a stable cold micro-plasma while avoiding the electric arc.

One of the most widely used approaches to avoid the electrical arcs at atmospheric pressure is the DBD: a dielectric (electrical resistivity $\rho > 10^8 \Omega \cdot \text{cm}$) is used to cover at least one of the electrodes. One of the DBD limitations is that it needs to be operated with frequencies ranging from the kHz to the MHz. This requires special high voltage power supplies at those frequencies, which added complexity for operating system. This shortcoming was overcome by replacing the dielectric barrier by a high resistivity layer ($\rho < 10^8 \Omega \cdot \text{cm}$). Doing so allowed the extension of the frequency range all the way down to 0 Hz (DC). In this case, the device is known as a Resistive Barrier Discharge (RBD) [16-21].

In order to propose a simple assembly system, we tested in this work the feasibility of covering the electrodes with a high resistivity layer. A comparison is presented between two different layers: semi-conductive ($\rho_1 = 10^3 \Omega \cdot \text{cm}$) and semi-insulating ($\rho_2 = 10^6 \Omega \cdot \text{cm}$). Different designs of the head of the fiber with deposited layers are proposed and studied. For each case, the lifetime of the fiber-plasma technology is recorded. Characterizations were also performed such as the stability of the system, and the identification of generated species.

This technology combines the characteristics of optical fibers (several tens-of-meters micrometric tube, good mechanical properties), with the properties of plasma (partially ionized gas containing electrons, ions, atoms and molecules in the ground or excited state, radical species, and quanta of electromagnetic radiation). For that, the potential application areas of our technology are very diverse, such as the detection of gases and organic vapors [14, 22], the inactivation of bacteria [16-21], and the surface treatment of different materials (cleaning, coating, painting, and adhesive bonding) [23].

The paper is structured as follows. Section II describes the experimental setup. The results with discussions are presented in Section III. Finally, the last section summarizes the main achievements and the conditions for optimizing the operation of the fiber-plasma technology.

II Experimental setup

The multimaterial fiber is fabricated by the direct preform-to-fiber drawing method. It is a hollow cylindrical fiber composed of a $\sim 620\ \mu\text{m}$ polyether-sulfone (PES) cladding with a central hole of $\sim 150\ \mu\text{m}$ surrounded by two $\sim 50\ \mu\text{m}$ tin electrodes themselves separated by a $\sim 250\ \mu\text{m}$ gap. Details of the drawing process are described in reference [14]. Due to its mechanical properties, the fiber is easy to process and manipulate (connection of embedded electrodes, bending, etc.). Abrasive machining on both sides of the fiber is required to connect laterally the electrodes to a DC generator (Branderburg AlphaIII). The electrodes at the tip of the fiber were covered with resistive layers (porous ethylene-propylene rubber tape $\rho_1 = 10^3\ \Omega\cdot\text{cm}$, and porous polyvinyl chloride tape with adhesive rubber $\rho_2 = 10^6\ \Omega\cdot\text{cm}$) using a stereo microscope (OLYMPUS SZX10). To prevent unwanted discharges, the electrodes at the second tip of the fiber were covered with insulators (epoxy resin with $\rho' = 10^{15}\ \Omega\cdot\text{cm}$).

An optical system for imaging was mounted. A Sony alpha A7S II camera is coupled to a microscope objective 10X, using two lens tubes ($L = 5\ \text{cm}$), a plano-convex lens ($f = 5\ \text{cm}$) and corresponding adapters. The system is connected to a software (Imaging Edge) to process the photos. The sketch of the experimental setup is shown in Fig.1.

By applying a potential of 1.2 kV, an air micro-plasma is generated at the tip of the fiber between electrodes. Plasma radiation is collected and then injected into a circle-to-linear bundle detector of 19 optical fibers (each fiber is 2 m long and has a $100\ \mu\text{m}$ core diameter) by a 5 cm converging lens and finally introduced into a Czerny-Turner spectrometer (Kymera 328i, Andor) equipped with a 1200 l/mm grating blazed at 300 nm. An intensified CCD camera (iStar CCD 340, Andor) enables the tuning of the delay and gate parameters, as well as the gain, for signal amplification.

The DC electric current is measured using a multimeter placed between the fiber and the generator (see Fig.1).

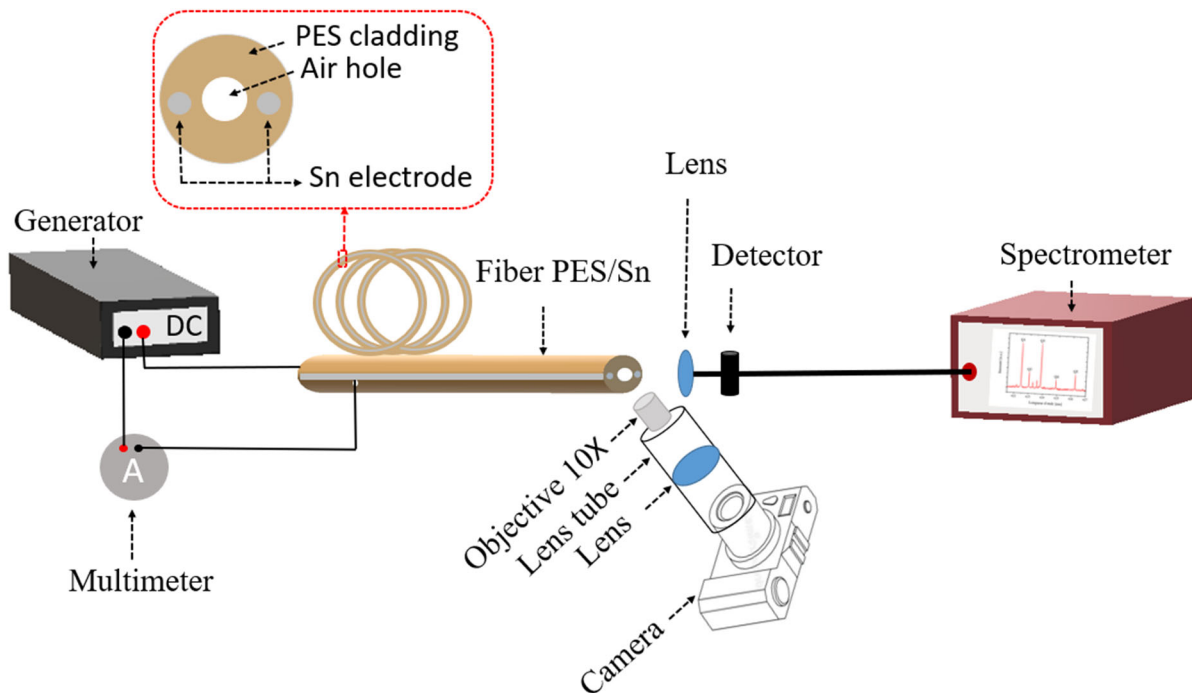


Fig.1. Sketch of the experimental setup.

III Experimental results and discussion

In order to optimize the operation and improve our technology, studies focus on the modification of the electrical properties of the fiber by covering the electrodes with resistive layers (section 3.1). Characterizations were also performed for the system (section 3.2), such as the stability (3.2.1), and the identification of generated species (3.2.2).

3.1 Optimization of the fiber-plasma technology

Previous studies have shown the ability of the RBD to generate a stable cold plasma at atmospheric pressure [16-21]. This discharge is somewhat similar to the DBD configuration, but instead of a dielectric barrier ($\rho > 10^8 \Omega \cdot \text{cm}$), a high resistivity layer ($\rho < 10^8 \Omega \cdot \text{cm}$) is used to cover at least one of the electrodes. The high resistivity sheet plays the role of a distributed resistive ballast, which helps avoid the discharge from localizing and inhibits the current from increasing to high values and turning the discharge into an electrical arc [16].

In order to study the effect of the resistive layer for our discharge, the electrodes at the tip of the fiber were covered with resistive layers. Three different designs of the fiber head are proposed and studied (D1, D2, and D3, see Fig.2). A comparison between two different layers is also presented: semi-conductive layer ($\rho_1 = 10^3 \Omega \cdot \text{cm}$) and semi-insulating layer ($\rho_2 = 10^6 \Omega \cdot \text{cm}$).

As shown in Fig.2, D1 presents the fiber head without adding any resistive layer; this is the same design used in reference [14].

For D2, the electrodes were covered with semi-conductive layers. D3 has the same shape as D2 but using semi-insulating layers.

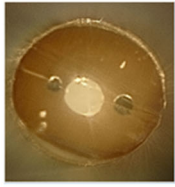
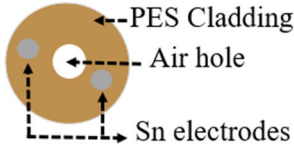
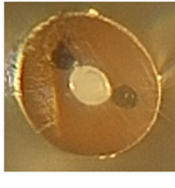
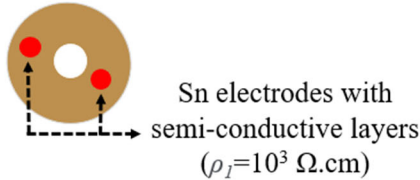
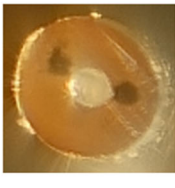
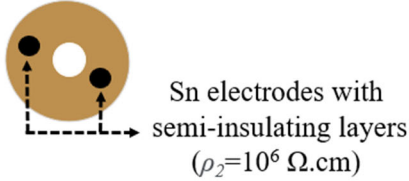
Design	Photo	Sketch
D1		
D2		
D3		

Fig.2. Photo and sketch for the fiber head for different designs (D1, D2, and D3).

By applying a DC voltage of 1.2 kV, the plasma is generated between electrodes for all designs of fibers. The lifetime of fiber-plasma technology is recorded for each case. For each design, the experiment was repeated four times using different fibers (four tests presented in Fig.3). We define t_{test} as the overall duration of the performed experiments, in this section $t_{test} = 240$ min.

As shown in Fig.3, for all performed tests, the lifetime is only a few minutes for designs D1 and D2. The electrodes are totally degraded after discharge. However, for design D3, the fibers remained functional after four hours (240 minutes) of discharge without damaging the electrodes.

Indeed, for D1 and D2, the glow discharge is turned into an electric arc. So, the semi-conductive layer is not effective to avoid it. However, based on the results of D3, we can conclude that the deposition of the semi-insulating layers on the electrodes allows to prevent their degradation, and increase the lifetime of fiber-plasma technology by at least 24 times. So, we have shown the efficiency of the RBD for a novel plasma reactor (using optical fiber), and greatly improve the lifetime of our technology.

It should be noted here that the duration of experiments is limited to four hours (240 min) because it is sufficient for most applications [16]. However, as we were able to generate a RBD with the fiber using the design D3, we can expect a permanent discharge as shown in references [16-21].

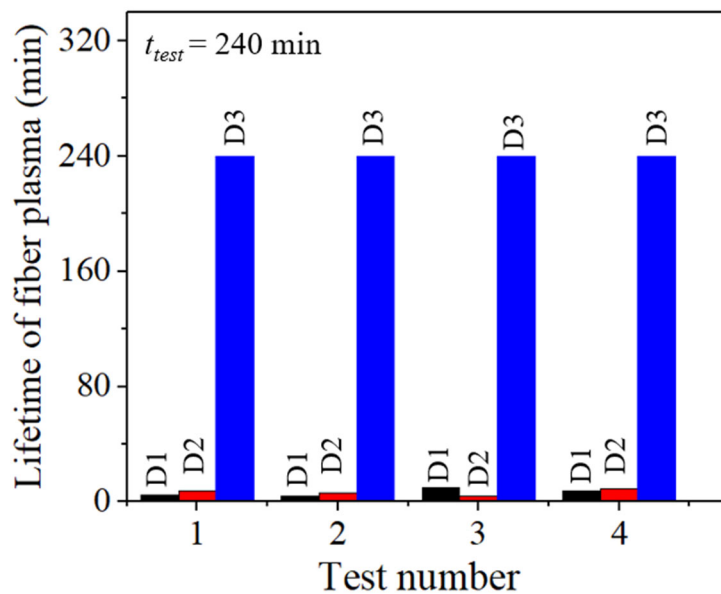


Fig. 3. Lifetime of the fiber-plasma technology for the designs D1, D2, and D3 measured for four different tests ($V_a=1200$ V, $t_{test}=240$ min).

On the other hand, for design D3, we noticed that the plasma moved far from the central position. For this reason, and in order to direct the plasma to a less resistive and shorter path, we proposed a final design, noted D4. For design D4, only one electrode was covered with the semi-insulating layer, and two semi-insulating layers are also deposited on both sides of the second electrode as shown in Fig.4 (a). The fiber remained functional after four hours of discharge (240 minutes) without damaging the electrodes as the case of design D3. So, we can conclude that the deposition of the semi-insulating layers on at least one electrode is sufficient to prevent the electric arcs. On the other hand, the deposition of semi-insulating layers on both sides of the second electrode facilitated the stabilization of the plasma position between electrodes during discharge. Photos of plasma during different times of the discharge using design D4 are shown in Fig.4 (b). Plasma remains in the same position and well centered between the electrodes at different times of discharge. For that, the following studies were carried out using this design.

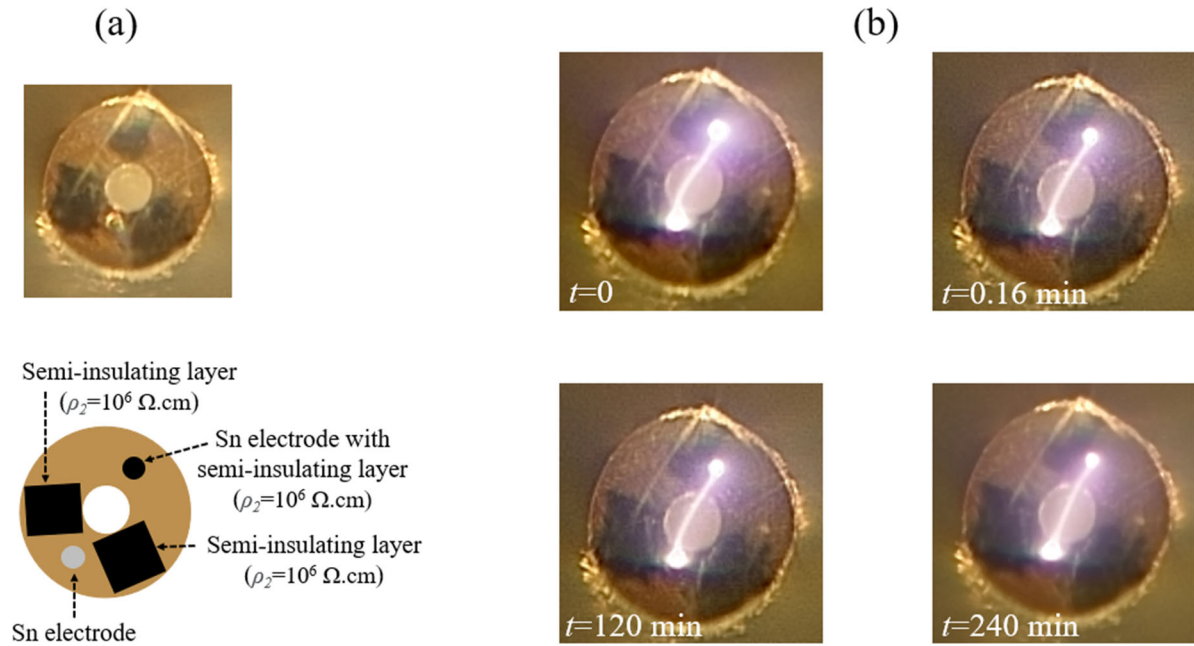


Fig.4. (a): Photo and sketch for the fiber head for design D4, (b): photos of the fiber head at different times of the discharge ($V_a=1200$ V, $t_{test}=240$ min, design D4).

3.2. Characterization of the fiber-plasma technology

3.2.1 Stability of the system

To study the stability of the system for different applied voltage (V_a), two values are compared in this section (1200 and 1600 V). As shown in Fig.5 (a), for $V_a = 1600$ V the plasma appears brighter, but it is still well centered between the electrodes. We have also measured the DC electric current for each voltage. As expected, it is higher for 1600 V (see Fig.5 (b)). Indeed, the current is directly proportional to the number of electrons, and a higher applied voltage increases the number of charged particles in the plasma (electrons and ions). As shown in Fig.5 (b), for both voltages, the current increases only during the first tens of seconds, then it remains constant until the end of the experiments ($t_{rest} = 180$ min), which shows a stable discharge for both cases.

On the other hand, a voluntary cycling study is also presented. The cycling ratio is defined by dividing the active time by the period. An example, for a ratio of 0.75 is shown in Fig.6. For the active times, noted ON ($V_a = 1200$ V), the plasma is generated and well centered between electrodes, the electrical current increases during the first tens of seconds, and it remains constant with a value of $30 \mu\text{A}$ (± 2). It is turned zero during the inactive time, noted OFF in Fig.6 ($V_a = 0$ V).

So, we have shown the stability of our device with a continuous discharge up to a few hours (Fig.5) or with a cycling ratio (Fig.6). We have also demonstrated the reproducibility of the discharge generated by measuring the same value of electric current for the same voltage ($V_a = 1200$ V and $i \approx 30 \mu\text{A}$ see Fig.5 (b) and 6).

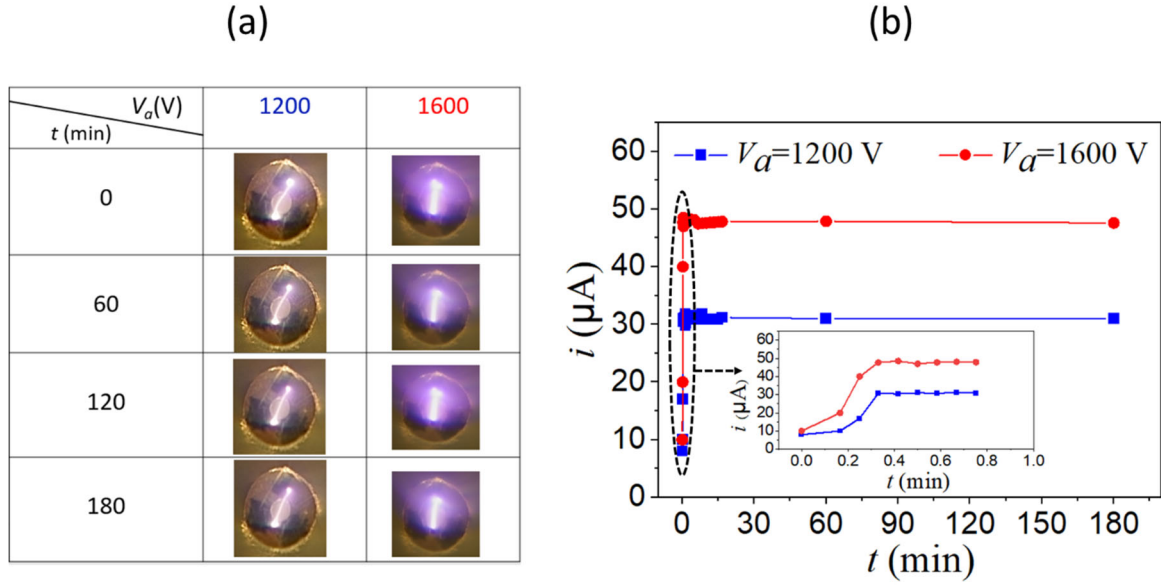


Fig.5. (a): Photos of the fiber head at different times of discharge; (b): temporal evolution of the electric current ($V_a = 1200$ and 1600 V, $t_{test} = 180$ min).

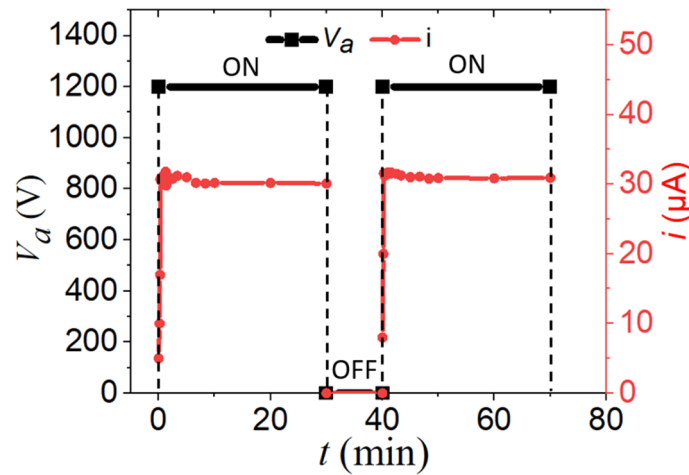


Fig.6. Temporal evolution of the applied voltage (V_a) and the electric current (i) with a voluntary cycling ratio of 0.75.

It should be noted here that the length of the hybrid fiber PES/Sn is monitored during drawing process. Several tens-of-meters of polymer metal structure can be fabricated. Before the plasma experiments, we have checked for each fiber the continuity of the electrodes by measuring the electrical resistance (the circuit was closed using silver lacquers). We tested the cases of fibers with different lengths from a few centimeters to a few meters. All fibers remained functional and showed a same behavior. We can conclude that the plasma properties depend on the continuity of the electrode along the fiber, the deposited resistive layers, and the applied voltage but not on the length of the fiber.

3.2.2 Identification of generated species

According to the Optical Emission Spectroscopy (OES), the species generated by the fiber-plasma device are identified. The optical spectrum is shown in Fig.7. It shows emission lines of OH(A-X) (~309 nm), various of the second positive system (SPS) of N_2 (300-450 nm), the first negative system (FNS)

of N_2^+ (350-450 nm), and the atomic line $H\alpha$ (656.3 nm). The spectrum is dominated by the peaks related to the N_2 and N_2^+ , mostly due to the very high concentration of molecular nitrogen in air atmosphere [24].

Atmospheric pressure air plasma is an attractive technology because it is easy to set up and handle, low-cost and safe. The progress in using air reduced the need for noble gases to be used as working gas to generate plasma without affecting its effectiveness. Therefore, in recent years, the interest in the production of this plasma has increased significantly [25-27]. To contribute to these advancements, in this work, we propose a high flexible new reactor based on hybrid fibers.

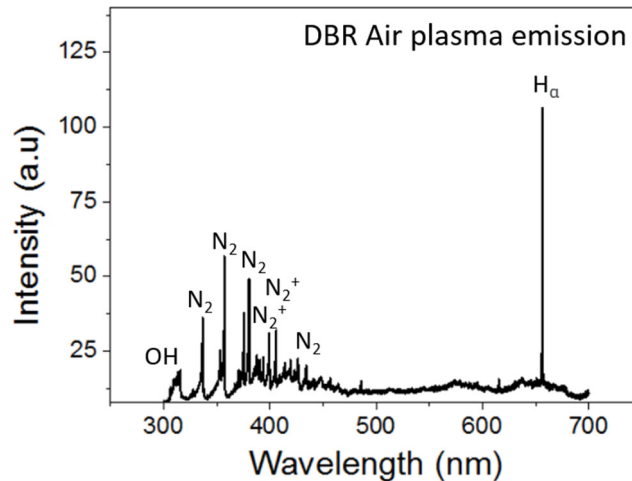


Fig.7. Optical emission spectrum of the air plasma ($V_a = 1200 V$).

IV Conclusion

In the context of the development of hybrid multi-purpose optical fibers, this work is devoted to optimize the operation of an innovative technology based on the combination of multimaterial fibers and plasmas. The fiber is composed of a polymer cladding with a central hole surrounded by two metal electrodes. By applying a DC voltage between the electrodes, an air micro-plasma is generated at its tip at atmospheric pressure. To improve the lifetime and the stability of our discharge and prevent the degradation of the electrodes, a deposition of high resistive layers was performed. Different designs of the fiber head with deposited layers are presented and studied. Characterizations were also performed for the fiber-plasma device such as the stability and the identification of generated species. These studies allow to increase considerably the lifetime of the technology and generate a cold stable air micro-plasma. This class of composite builds allows the emergence of novel applications for fibers, such as sterilization and decontamination of medical equipment, various surface treatment or gas detection.

Funding: This work has received support from the University of Bordeaux (Grant n°OPE-2021-0383) and from the European Union’s Horizon 2020 research and innovation programme under the Marie Skłodowska-Curie grant agreement No 823941 (FUNGLASS).

Data availability: The data that support the findings of this study are available from the corresponding author upon reasonable request.

Conflicts of Interest: The authors declare no conflict of interest in the subject matter or materials discussed in this manuscript. Authors have no affiliation with any organization with a direct or indirect financial interest in the subject matter discussed in the manuscript.

References

- [1] Abouraddy, A.F.; Bayindir, M.; Benoit, G.; Hart, S.D.; Kuriki, K.; Orf, N.; Shapira, O.; Sorin, F.; Temelkuran, B.; Fink, Y. “Towards multimaterial multifunctional fibres that see, hear, sense and communicate”. *Nat. Mater.* 6, 336–347 (2007).
- [2] Strutynski, C.; Desevedavy, F.; Lemièrre, A.; Jules, J.-C.; Gadret, G.; Cardinal, T.; Smektala, F.; Danto, S. “Tellurite-based core-clad dual-electrodes composite fibers”. *Opt. Mater. Express* 7, 1503–1508 (2017).
- [3] Strutynski, C.; Alvarado Meza, R.; Teulé-Gay, L.; El-Dib, G.; Poulon-Quintin, A.; Salvetat, J.-P.; Vellutini, L.; Dussauze, M.; Cardinal, T.; Danto, S. “Stack-and-draw applied to the engineering of multimaterial fibers with noncylindrical profiles”. *Adv. Funct. Mat.* (2021).
- [4] Lee, K.; Hu, P.; Blows, J. L.; Thorncraft, D.; and Baxter, J. “200-m optical fiber with an integrated electrode and its poling”. *Opt. Lett.* 29(18), 2124–2126 (2004).
- [5] Dai, Y.; Du, M.; Huang, L.; Zheng, J.; Wei, L.; Qiu, J.; Ren, C.; Zhou, S. “Multimaterial Glass Fiber Probe for Deep Neural Stimulation and Detection”. *Adv. Optical Mater* 11, 2202184 (2023).
- [6] Xiao, X.; Le Berre, S.; Fobar, D.G.; Burger, M.; Skrodzki, P.J.; Hartig, K.C.; Motta, A.T.; Jovanovic, I. “Measurement of chlorine concentration on steel surfaces via fiber-optic laser-induced breakdown spectroscopy in double-pulse configuration. *Spectrochim. Acta Part B At. Spectrosc.* 141, 44–52 (2018).
- [7] Marquardt, B.J.; Goode, S.R.; Michael Angel, S. “In situ determination of lead in paint by laser-induced breakdown spectroscopy using a fiber-optic probe”. *Anal. Chem.* 68, 977–981 (1996).
- [8] Rai, A.K.; Zhang, H.; Yueh, F.Y.; Singh, J.P.; Weisburg, A. “Parametric study of a fiber-optic laser-induced breakdown spectroscopy probe for analysis of aluminum alloys”. *Spectrochim. Acta Part B At. Spectrosc.* 56, 2371–2383 (2001).
- [9] Whitehouse, A.I.; Young, J.; Botheroyd, I.M.; Lawson, S.; Evans, C.P.; Wright, J. “Remote material analysis of nuclear power station steam generator tubes by laser-induced breakdown spectroscopy”. *Spectrochim. Acta Part B At. Spectrosc.* 56, 821–830 (2001).
- [10] Cremers, D.A.; Barefield, J.E.; Koskelo, A.C. “Remote Elemental Analysis by Laser-Induced Breakdown Spectroscopy Using a Fiber-Optic Cable”. *Appl. Spectrosc.* 49, 857–860 (1995).
- [11] Zuo, X.; Wei, Y.; Wei Chen, L.; Dong Meng, Y. “Non-equilibrium atmospheric pressure microplasma jet: An approach to endoscopic therapies”. *Phys. Plasmas* 20, 083507 (2013).
- [12] Kim, J.Y.; Wei, Y.; Li, J.; Foy, P.; Hawkins, T.; Ballato, J.; Kim, S.O. “Single-cell-level microplasma cancer therapy”. *Small* 7, 2291–2295 (2011).
- [13] Kim, J.Y.; Ballato, J.; Foy, P.; Hawkins, T.; Wei, Y.; Li, J.; Kim, S.O. “Apoptosis of lung carcinoma cells induced by a flexible optical fiber-based cold microplasma. *Biosens.* *Bioelectron.* 28, 333–338 (2011).
- [14] Strutynski, C.; Teulé-Gay, L.; Danto, S.; Cardinal, T. “Optical emission detector based on plasma discharge generation at the tip of a multimaterial fiber”. *Sensors* 20, 2353 (2020).
- [15] Schutze, A.; Jeong, J. Y.; Babayan, S. E.; Park, J.; Selwyn, G. S.; and Hicks, R. F. “The Atmospheric-Pressure Plasma Jet: A Review and Comparison to Other Plasma Sources”. *IEEE Transactions on plasma science*, vol. 26, No. 6 (1998).

- [16] Laroussi, M. “The Resistive Barrier Discharge: A Brief Review of the Device and Its Biomedical Applications”. *Plasma* 4, 75–80 (2021).
- [17] Thiyagrajan, M.; Alexeff, I.; Parameswaran, S.; Beebe, S. “Atmospheric pressure resistive barrier cold plasma for biological decontamination”. *IEEE Trans. Plasma Sci.* 33, 322 (2005).
- [18] Laroussi, M.; Richardson, J.P.; Dobbs, F.C. “Effects of Non-Equilibrium Atmospheric Pressure Plasmas on the Heterotrophic Pathways of Bacteria and on their Cell Morphology”. *Appl. Phys. Lett.* 81, 772 (2002).
- [19] Laroussi, M.; Mendis, D.A.; Rosenberg, M. “Plasma Interaction with Microbes”. *New J. Phys.* 5, 41 (2003).
- [20] Thiyagrajan, M.; Alexeff, I.; Parameswaran, S.; Beebe, S. “Atmospheric pressure resistive barrier cold plasma for biological decontamination”. *IEEE Trans. Plasma Sci.* 33, 322 (2005).
- [21] Uhm, H.S.; Kang, J.G.; Choi, E.H.; Cho, G.S. “Sterilization of medical equipment and contaminated articles by making use of a resistive barrier discharge”. *J. Korean Phys. Soc.* 61, 551 (2012).
- [22] Vincent, J.; Wang, H.; Nibouche, O.; and Maguire, P. “Detecting trace methane levels with plasma optical emission spectroscopy and supervised machine learning”. *Plasma Sources Sci. Technol.* 29 085018 (2020).
- [23] Yi, C.H.; Lee, Y.H.; Yeom, G.Y. “The study of atmospheric pressure plasma for surface cleaning”. *Surface and Coatings Technology*, Volume 171, Issues 1–3 (2003).
- [24] Misra, N.N.; Ziuzina, D.; Cullen, P.J.; Keener, K.M. “Characterization of a novel atmospheric air cold plasma system for treatment of packaged biomaterials”. *Trans. ASABE* 56, 1011–1016 (2013).
- [25] Gerber, I. C.; Mihai, C.T.; Gorgan, L.; Ciorpac, M.; Nita, A.; Pohoata, V.; Mihaila, I.; Topala, I. “Air dielectric barrier discharge plasma source for in vitro cancer studies”. *Clin. Plasma Med.* 9, 4 (2018).
- [26] Xiao D.; Cheng, C.; Lan, Y.; Ni, G.H.; Shen, J.; Meng, Y.D.; Chu, P.K. “Effects of Atmospheric-pressure nonthermal nitrogen and air plasma on bacteria inactivation”. *IEEE Trans. Plasma Sci.* 44 2699–2707 (2016).
- [27] Dong X.Y. and Yang Y.L. “A novel approach to enhance blueberry quality during storage using cold plasma at atmospheric air pressure”. *Food Bioprocess Technol* 12 1409–1421 (2019).